J. Chem. Soc. Nigeria, Vol. 46, No.2, pp 0217 – 0224 [2021]

Bioremediation of Ni^{2+}, Cd^{2+} and Pb^{2+} from aqueous solution using chemically modified *Newbouldia Leavis* seed pod. Kinetics and Intraparticle Diffusivities.

O.K. Amadi[1]*, F.K. Ekuma[1] and B. N. Uche[1]
[1]Department of Chemistry, Michael Okpara University of Agriculture, Umudike, Umuahia, Abia State, Nigeria. P.M. B. 7267, Umuahia, Abia State.
*Corresponding Author: amadikelvin77@gmail.com., +234-08030745329
Received 11 February 2021 accepted 19 February 2021 published online 30 March 2021

Abstract:
This study investigates the biosorption of Ni^{2+}, Cd^{2+} and Pb^{2+} from aqueous solution by modified *Newbouldia Leavis* seed pod. The modification was done by acid treating air-dried activated *Newbouldia Leavis* seed pod by dissolving it in excess 1.0 M Mercapto acetic acid ($HSCH_2COOH$) solution, stirred for 30 minutes and left to stand for 24 hours at 30 ^oC, filtered off using WhatmanNo. 41 filter paper and were air dried. The effects of solution pH and contact time were evaluated. The results showed that maximum Cd^{2+} and Ni^{2+} adsorption of 7.9872 mg/g and 7.9809 mg/g respectively occurred at pH of 6.0 while that of Pb^{2+} was 8.0000 mg/g, at a pH of 4.0. The optimum time for maximum adsorption of the three heavy metal ions were 110 min. The kinetic data revealed that the sorption process could best be described by the pseudo – second order kinetic model. The R^2 values for the pseudo – second order kinetic plots were unity and were higher than first order reversible model and pseudo – first order plots. Moreover, the values of q_{cal} and q_{exp} obtained for pseudo – second order plots were very close indicating that the biosorption process followed the pseudo-second order kinetics. However, the transport mechanism for the process involved both intra-particle and liquid film diffusion.
Key Words: Sorption kinetics, Thiolation, Heavy metal ions, *Newbouldia Leavis*

1.0 Introduction
Environmental pollution by toxic metals is a worldwide problem due to increased industrialisation. The metal ions are particularly problematic due to their accumulation in the food chain and their persistence in the environment [1]. Ni^{2+}, Cd^{2+} and Pb^{2+} are among the metals of concern. Cadmium, which is widely used and extremely toxic in relatively low dosages, is one of the principal heavy metals responsible for causing kidney damage, renal disorder, high blood pressure, bone fraction and destruction of red blood cells [2]. Because of its toxicity and bioaccumulation, Cd^{2+} is considered as a priority pollutant by the U S Environmental Protection Agency. The permissible limit for Cd^{2+} as described by WHO is 0.01 mg/dm^{-3} in drinking water[3]. The main anthropogenic pathway through which Cd^{2+} enters the water bodies is via wastes from industrial processes such as electroplating, plastic manufacturing, metallurgical processes, pigment industries of and Cd/Ni batteries [4]. Nickel is found in a large variety of products such as automobiles, batteries, jewellery, surgical implants, kitchen appliances, sinks and utensils [5]. It is regarded as one of the essential trace elements for humans, plants and animals but it causes toxicity to aquatic life at higher concentrations [5]. Although lead occur naturally in the environment, anthropogenic activities such as fossil fuel burning, mining and manufacturing contribute to the release of high concentrations of lead. At very high concentrations, lead may cause structural damage to cells, proteins, nucleic acid, membranes and lipids, resulting in a stressed situation at cellular level [6]. There are several methods for removing heavy metals from wastewater. Some of these methods include chemical precipitation, ion exchange, electrochemical treatment, membrane technologies and adsorption among others [7]. However, some of these methods are expensive and may produce harmful by-products [8]. Numerous studies have demonstrated that modified agricultural by products have the ability to remove heavy metals from wastewater with better performance and lower cost compared with conventional technologies [9, 10, 11]

In this work, we investigated the kinetics of sorption of Cd^{2+}, Pb^{2+} and Ni^{2+} on modified *Newbouldia Leavis* pod. Reversible first order, pseudo first-order, pseudo second-order,

models were used to ascertain the rate kinetics for the sorption process. We also investigated the mode of diffusion by employing the various models involving intraparticle and liquid film diffusion models. Our aim was to generate data that could be used to effectively design sorption treatment plant for heavy metal removal from aqueous medium.

Materials and methods

Preparation of the adsorbent:

The adsorbent, *newbouldia leavis* pod was obtained at Michael Okpara University of Agriculture, Umudike, Abia state Nigeria. The pods were carefully removed, washed with de-ionized water, dried and crushed with a blender. The crushed samples were sieved to obtain 0.15 mm mesh size. The sieved samples were soaked in 0.3 M HNO_3, stirred for 30 min and left undisturbed for 24 h. They were then filtered through Whatman no. 41 filter paper and rinsed thoroughly with de-ionized water and sundried for 2 h. The adsorbent was kept in an oven at 105 ºC for 2 h and finally stored in a tight plastic container.

Chemical modification of *newbouldia leavis* pod with mercapto-acetic acid.

The air-dried activated *newbouldia leavis* pod were acid treated by soaking in excess of 1.0M Mercapto acetic acid ($HSCH_2CO_2H$) solution, stirred for 30 minutes and left for 24 hr at 28 ^oC . After 24 hr, the mixtures in the beaker named chemical modified *newbouldia leavis* pod were filtered off using Whatman No. 41 filter paper. The residue was then soaked in 1.0 M hydroxylamine (NH_2OH) for 1 h ro remove all 0-acetyl groups. After which they were filtered and rinsed with excess deionised water until a pH 6.8 was obtained. The washed residues were air dried and stored in an air tight container. The mercaptoacetic acid modification led to the thiolation of the hydroxyl groups of the biosorbents by the following reaction[9].

Biomass + $HSCH_2CO_2H \rightarrow$ Biomass-SH + $H_3CCO^-_2 + H^+$.

The degree of infusion of thiol (-SH) group was further estimated by reacting 0.5 g of acid treated biosorbents with 25 mL of iodine solution at pH 7.3, followed by back titration of the unreacted iodine with standard thiosulphate solution.

Instrumentation

Infrared spectra were obtained by using a Fourier transform infrared spectrometer (FTIR) (Perkin-Elmer Analyst 200). The analysis was performed to confirm the presence of surface functional groups. The powder samples (99 mg) were mixed well with 1 mg of potassium bromide (KBr) and pressed into pellets under vacuum, until they appeared clear and not translucent. The pellets were then carefully removed from the disc, placed in the FTIR sample holder and analyzed by the transmission mode with a resolution of 4 cm^{-1}. The spectra of the different samples were recorded in the wavenumber range of 4000 to 400 cm^{-1}.

Adsorption Experiments

Batch adsorption studies for the removal of Ni^{2+}, Cd^{2+} and Pb^{2+} by modified *newbouldia leavis* pod were investigated as a function of solution pH and contact time. The effect of solution pH on the adsorption of the metal ions was studied at a fixed temperature of 30 ^oC and at an initial metal ion concentration of 50 mg/L. The adsorption was carried out using varying pH of the solution ranging from 2 to 8. This was done by introducing 50 cm^3 of each metal ion solution into different 250 cm^3 Erlenmeyer flasks containing 0.05 g of the adsorbent and adjusting the pH of the solutions to 2, 4, 6, 7 and 8. The mixtures were agitated intermittently for 110 min in a rotary shaker and then filtered. The concentration of each filtrate was determined using Perkin Elmer Analyst 200 Atomic Absorption Spectrophotometer. The effect of contact time on adsorption of the metal ions was studied using the same method but at constant adsorbent mass of 0.05 g and constant pH of 4 for Pb^{2+} but 6 for both Cd^{2+} and Ni^{2+} solutions. However, the time was varied. From the results of the analysis, percentage removal of heavy metal ions by the adsorbents as well as the amount absorbed at a given time interval and the equilibrium amount adsorbed at different pH were calculated using equations 1 and 2 [12]

$$\%R = \frac{C_o - C_t}{Co} \times \frac{100}{1} \quad \text{----------(1)}$$

$$q_t = \frac{C_o - C_t}{1} \times \frac{v}{m} \quad \text{----------(2)}$$

where % R is the percentage of concentration of metal ion adsorbed, C_o = initial metal ion concentration in mg/L, C_t = residual metal ion

concentration in solution at time t (mg/L), V = volume of metal ion solution used in dm^3 and m the dry mass of the adsorbent in (g).

3.0 Results and Discussion

FT-IR Result: Both spectra depict high intensity broad peaks observed at 3398.32 cm^{-1}, 2924.8 cm^{-1} caused by both the O–H stretching vibration and C–H stretching vibration of alkyl (–CHn) groups contained in lignin. Special emphasis goes to the –SH stretching vibration (2345.6 cm^{-1}) as it depicts the grafting of sulfydryl groups onto the adsorbent. The peaks observed at 1722.7 cm^{-1} and 1633.45 cm^{-1} correspond to $C{=}O_{st}$ and $C{=}O_{asy}$ respectively [13]. The band at 1384.87 cm^{-1} is assigned to $C–H_{df}$. The peak at 1282.30 cm^{-1} is ascribed to vibrations of both $C{=}O_{df}$ and $-OH_{st}$ is assigned to $C–O_{st}$ [13]. From Figs.1 and 2, intensity shifts, disappearances, increase or decrease at some bands are observed. The disappearance of 1722.7 cm^{-1} band in Fig. 2 suggests $C{=}O_{st}$ as a possible point of chelation. Moreover, the decrease in intensities from 2345.6 to 2115.5 cm^{-1} suggested that the sulfydryl group moderately chelates with the metal ions. However, increase in O–H stretching vibrations from 3398.32 cm^{-1} to 3435.95 cm^{-1}, suggests non chelation at O–H [14].

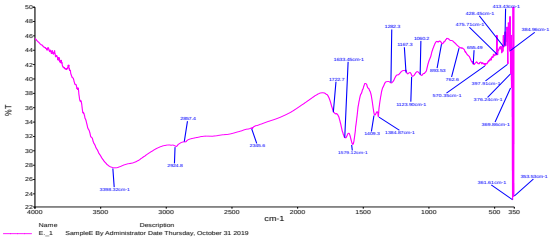

Fig. 1: FTIR spectrum of the adsorbent before adsorption.

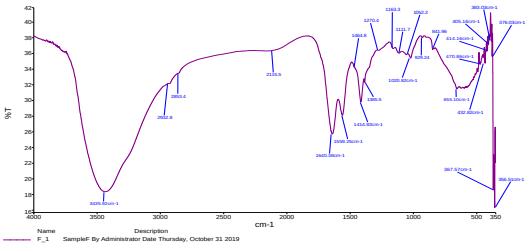

Fig. 2: FTIR spectrum of the adsorbent after adsorption.

Effects of pH variation

The pH of a solution can affects the surface charge of the adsorbent, as well as the degree of the ionization and speciation of different pollutants [12]. The plots in Fig. 3 reveal that the amount of the heavy metal ions adsorbed increases with increase in pH up to 4 for Pb^{2+} but up to 6 for Ni^{2+} and Cd^{2+} before decreasing. Therefore, the maximum adsorption capacities at the above mentioned pH for $Pb^{2+,}$ Cd^{2+} and Ni^{2+} are 7.9894 mg/g 7.9381 mg/g and 7.8889 mg/g respectively. This reveals that the adsorption of the metal ion strongly favours acidic pH than alkaline pH. At low pH, the adsorption sites are populated by hydroxonium ion but as the pH increases, the hydrogen ions are gradually depleted from the surface of the adsorbent leading to corresponding increase in the amount of heavy metal ions adsorbed. However, at critical pH (i.e pH = 6), the proportion of the adsorption sites that was activated reduces due to increase in concentration of hydroxyl ion and the formation of insoluble $Pb(OH)_2$, $Cd(OH)_2$ and $Ni(OH)_2$ [15]. Hence, the amount of heavy metal ion adsorbed remains constant until further decrease in pH that will enhance desorption or precipitation [16]. Hence, the optimum pH for the adsorption of Cd^{2+} and Ni^{2+} is pH 6 but pH 4.0 for Pb^{2+} accordingly and was used for the rests of the study.

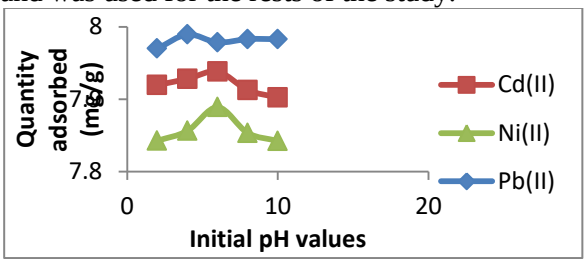

Fig. 3: Effect of pH on biosorption oheavy metal ions onto *Newbouldia Leavis* pod.

Effect of contact time

The sorption of the metal ions was determined as a function of time to determine an optimum contact time for equilibrium sorption of the metal ions onto the sorbent. Fig. 4 is a plot that shows the variation of the metal ions adsorbed by adsorbent with time. The plots reveals that the uptake of the metal ions witnessed a sharp initial increase (up to 30 minutes) and then gradually becoming constant for the adsorbent up to 110 min (critical time). The observed trend can be explained in terms of increase in diffusion rate and active adsorption site at first but after the critical time, active adsorption sites have been occupied, giving way to distortion of

adsorption-desorption equilibrium [17]. However, after the critical time, the adsorption approached equilibrium and remains constant.

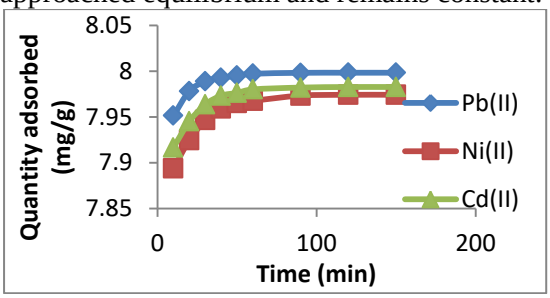

Fig. 4: Variation of the amount of metal ion adsorbed with time

Adsorption kinetics

It is necessary to identify the adsorption mechanism for a given adsorption system. Kinetic models have been exploited to test the experimental data and to find the mechanism of adsorption and its potential rate-controlling step that include mass transport and chemical reaction. Moreover, information on the kinetics of metal uptake is required to select the optimum conditions for full scale batch or continuous metal removal processes [18].

Pseudo first order model

The Pseudo first order rate model is based on adsorption capacity of adsorbent and is generally expressed [19]: $\frac{dq_t}{d_t}$ = k1(qe-qt) (3)

$\ln(q_e-q_t) = \ln qe - k_1 t$ (4)

Where, q_e and q_t are the amounts (mg/g) of the metal ions adsorbed at equilibrium and at time (t), respectively. Plot of $\ln(q_e-q_t)$ versus t should give a straight line for first order adsorption kinetics from which the computation of the rate constant k_1 is allowed

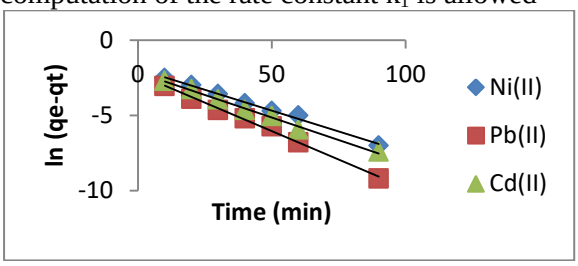

Fig. 5: Pseudo first order plot of ln(qe-qt) vs t for the adsorption of the metal ions onto *Newbouldia Leavis* pod

Pseudo-second order model

Pseudo-second order model is derived on the basis of adsorption capacity of the solid phase, expressed [20]: $\frac{dq_t}{d_t} = k_2(q_e-q_t)^2$ (5)

where k_2 is the rate constant of pseudo second-order adsorption (g/mg min), The integrated form of equation (5) within the boundary conditions is expressed in equation (6) as:

$$\frac{t}{q_t} = \frac{1}{k_2 q_e^2} + \frac{t}{q_e} \quad (6)$$

Consequently, equation 6 indicates that a plot of $\frac{t}{q_t}$ versus t should give a linear plot with slope and intercept equal to $1/q_e$ and $\frac{1}{k_2 q_e^2}$. The model also contain factors that enhance the estimation of the initial adsorption rate, ho (g/mg min) as t approaches zero, i.e $h_o = k_2 q_e^2$. The pseudo second order plots (Fig. 6) gave slopes and intercepts that lead to the estimation of the observed kinetic parameters, k_2 , q_e, h_o and R^2 which are recorded in Table 1.The half-adsorption time $t_{1/2}$ is also a significant adsorption parameter which can be calculated from the equilibrium concentration and the diffusion coefficient rate values. This was calculated by using the following equation 7 [21]: $t_{½} = \frac{1}{k_2 q_e}$ (7)

The experimental data for the adsorption of the metal ions onto the adsorbent were also employed to evaluate the controlling mechanism of adsorption processes. The diffusion coefficients for the intra-particle transport of the metal ions were calculated using equation 8 [22]: $D = \frac{0.03r^2}{t_{1/2}}$ (8)

where *r* is the radius of the adsorbent particle in (cm) and D is the diffusion coefficient value in ($cm^2.min^{-1}$). Estimated D values (Table 1) correlated with the equilibrium amount of heavy metal ion adsorbed. Lead which had best adsorption had the highest value of D accordingly.

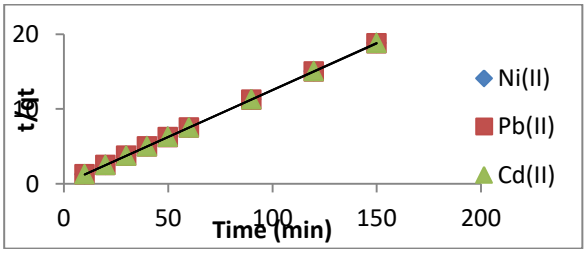

Fig.6: Pseudo second order plot of t/qt vs t for the adsorption of the metal ions onto *Newbouldia Leavis* pod

First order reversible reaction model

This model is mostly used for biosorption kinetics [23]. It can, however, describe the

adsorption and desorption phenomena simultaneously using rate constant parameters. This model assumes that adsorption of metal (A) on adsorbent (B) follows first-order reversible reaction. The integral form for the model is represented by:

$$-\ln\left[\frac{C_A - C_{Ae}}{C_{Ao} - C_{Ae}}\right] = (k_1 + k_2)t \qquad (9)$$

Where, k_1 and k_2 are rate constants for adsorption and desorption. The plot between $-\ln\left[\frac{C_A - C_{Ae}}{C_{Ao} - CAe}\right]$ vs t would be a straight line with slope of $(k_1 + k_2)$. The constants k_1 and k_2 are related to sorbate concentrationas:

$$\frac{k_1}{k_2} = \frac{X_{Ae}}{1 - X_{Ae}} = \frac{C_o - C_{Ae}}{C_{Ae}} \qquad (10)$$

Where, X_{Ae} is fraction adsorption at equilibrium. Hence, k_1 and k_2 can be computed and summarized in Table 1. Kinetics of the metal ions adsorption on the adsorbent is described well by Pseudo-first order rate model, first order reversible reaction model and Pseudo second order model. However, only the Pseudo second order model fits well having regression coefficient >0.9999. Further, it can be seen from Table 1 that the forward rate constant for the removal of the metal ions is much higher than the backward rate constant, namely the desorption process. The low value of k_2 (rate constant for desorption process) indicates that the adsorbed metal ions is relatively stable on the adsorbent at temperature and concentration studied.

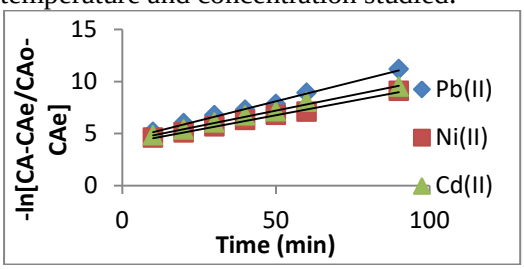

Fig. 7: First order reversible plot of $-\ln\left[\frac{C_A - C_{Ae}}{C_{Ao} - CAe}\right]$ vs t for the adsorption of the metal ions onto *Newbouldia Leavis* pod

Intraparticle diffusion model

According to this model, initial rate of the intraparticle-diffusion is given by the following equation [24].$qt = k_{in} t^{1/2} + I$ (11)

Where, k_{int} (mg/g-min$^{1/2}$) is the intraparticle-diffusion rate constant and qt (mg/g) is the amount of ions adsorbed at time t (min) while large I intercept suggests great boundary layer effect. A plot of qt versus $\sqrt{t}$ can give a linear or multilinear suggesting that intraparticle diffusion is involved in the adsorption process or two or more steps govern the adsorption process. However, if a linear graph is obtained and the plot passes through the origin then intraparticle diffusion is said to be the sole rate-limiting step. Fig. 8, shows that the plots are non linear but the double linear model obtained reveals that the adsorption is intra particle diffusion controlled. In this first straight line, a sudden increase in slope was observed which indicates that the metal ions are transported to the external of the adsorbent through film diffusion at a fast rate and was succeeded by penetration of the metal ion into the adsorbent. –However, both lines did not yield zero intercept which suggests that film diffusion and intra particle diffusion are occurring simultaneously during the adsorption. While ki_1, I_1 and $R^2_1$are the slope, intercept and correlation of the first steeper portion, ki_2, I_2 and R^2_2 indicates the slope, intercept and correlation of the second linear portion respectively. Since $ki_1 > ki_2$, it means that, both liquid film diffusion and intraparticle diffusion models are the rate limiting steps [25; 15].In equation (15), k_d (mg.g^{-1}.min$^{-1/2}$) is defined as the intraparticle diffusion rate constant and is related to the intraparticle diffusivity in the following way (12). $kint = \frac{6q_e}{r}\sqrt{\frac{D}{\pi}}$ (12)

where r (cm) is the particle radius, D (cm^2.min^{-1}) is diffusion coefficient, and qe (mg.g-1) is the solid phase concentration at equilibrium [26].

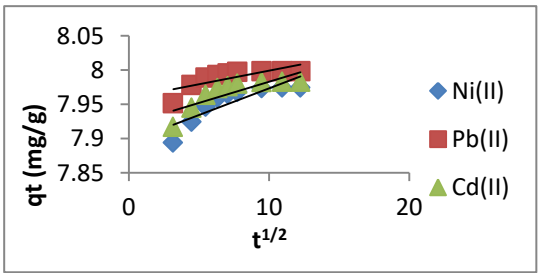

Fig. 8: Weber and Morris Intra particle diffusion model for the heavy metal ions adsorption onto *Newbouldia Leavis* pod.

Liquid film diffusion model

The film diffusion model, proposed by McKay (where kp is the rate constant for film diffusion, min^{-1}; F is the fractional attainment):

$\ln (1- F) = -k_p t + D_F$ (13)

Hence $F = \frac{q_t}{q_e}$ (14)

A plot of In(1-F) versus time (t) was linear as shown in Fig. 9. The rate constant K_p and dimensionless constant D_F are obtained from the slope and intercept respectively, The linearity of the plots confirms that film diffusion is involved in the metal ions adsorption. However, non displayed zero intercept suggests that both film diffusion and intra particle diffusion mechanism are the limiting steps in the adsorption processes. The thin liquid film may produce a diffusion barrier for the metal ions to penetrate before they arrive at the binding site on the adsorbent and must be overcome before adsorption [27]. In a particle diffusion controlled sorption process, the intra particle mass transfer resistance is the rate limiting step. That is, in the presence of a mixture of metal ions, competition for available adsorption sites will set in and the diffusion properties of the respective ions would be affected, hence the adsorption capacity of the individual metal ion will likely decrease. Consequently, the metal ion that successfully reaches the adsorption site faster must have satisfied several conditions more than others [28].

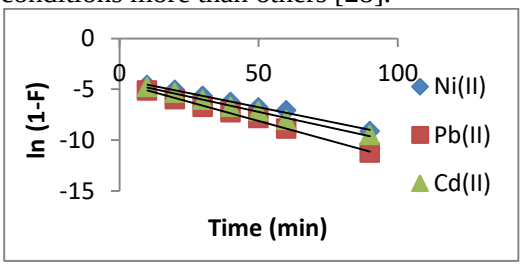

Fig. 9: Liquid film diffusivity model for adsorption of Pb(II), Cd(II) and Ni(II) ions adsorption onto *Newbouldia Leavis* pod

Table 1: Kinetic parameters for the adsorption of the heavy metal ions onto modified *newbouldia leavis* seed pod. Considering r = 0.009 cm. $t_{1/2}$ was calculated from (7) considering r = 0.009 cm

Adsorption Kinetic models	Parametes	Pb^{2+}	Cd^{2+}	Ni^{2+}
Reversible first order	K_1 (min^{-1})	0.074	0.059	0.055
	K_2 (min^{-1})	1.547 x 10^{-5}	12.886 x 10^{-5}	17.904 x 10^{-5}
	X_{Ae}	0.999	0.997	0.996
	R^2	0.994	0.994	0.995
Pseudo First-Order	q_{cal} (mg/g)	0.102	0.1153	0.1468
	q_{exp} (mg/g)			
	k_1 (min^{-1})	0.075	0.060	0.055
	R^2	0.994	0.995	0.995
Pseudo Second-Order	q_{cal} (mg/g)	8.000	7.987	7.981
	q_{exp} (mg/g)	7.998	7.983	7.974
	k_2($dm^3 mol^{-1} min^{-1}$)	2.604	1.474	1.075
	h_o(g/mgmin)	166.667	94.340	68.493
	t½ (min)	0.048	0.085	0.117
	D ($cm^2.min^{-1}$)	5.063 x 10^{-5}	2.861 x 10^{-5}	2.086 x 10^{-5}
	R^2	1.000	1.000	1.000
Elovich	α (mg/g)	8.274	2.297	3.062
	β(g mgmin)	64.103	42.194	33.784
	R^2	0.777	0.842	0.879
Weber and Morris intraparticle diffusion	C_{i1} ($mg.g^{-1}$)	7.923	7.872	7.839
	k_{i1} ($mg.g^{-1}$ $min^{-1/2}$)	0.011	0.016	0.019
	R_i^2	0.891	0.954	0.974
	C_{i2} ($mg.g^{-1}$)	1.993	7.971	7.954
	k_{i2} ($mg.g^{-1}$ $min^{-1/2}$)	0.001	0.001	0.002
	R_2^2	0.666	0.733	0.847
Liuid Film Diffusion Model	K_p	0.075	0.060	0.056
	D_F	-4.376	-4.238	-3.987
	R^2	0.994	0.995	0.994

Conclusion

In this study, *Newbouldia Leavis* pod was used for the biosorption of the aqueous solution of Cd^{2+}, Ni^{2+} and Pb^{2+} ions. Batch experiment showed that the solutions pH strongly influenced the biosorptive capacity of the adsorbent. As the solution pH increased, the equilibrium sorption capacity of Ni^{2+}, Cd^{2+} and Pb^{2+} increased. However, optimum pH for maximum adsorption was 6 and occurred within the first 110 minutes for Cd^{2+}, Ni^{2+} and Pb^{2+}. A pseudo second order kinetic model provided better data than first order reversible model and pseudo first order model. This study validates that the adsorbent could be used as inexpensive and highly efficient reliable biosorbent for effectively removing heavy metal ions from aqueous solution.

Reference

[1] B.Y.M., Bueno, M. L.,Torem, F., Molina & L. M. S. Mesquita.(2008). Biosorption of lead (II), chromium (II) and copper (II) by *R.opacus*: equilibrium and kinetic studies. *MineralsEng*. 21(1): 65 -75

[2] O.K. Amadi, A. Okoyeagu, & O.U. Akoh.(2020). Biosorption of Pb(II), Ni(II) and Cd(II) ions from aqueous phase by Ceaser weed (*Urena Lobata*) bark, a low cost biosorbent. *J. Chem. Soc. Nigeria*, 45 (4); 580 -586

[3] U. Guyo, T Makawa, M Moyo, T Nharingo, B C Nyamunda, and T Mugadza (2015) *Journal of Environment Chemical Engineering* 3; 2472-2483

[4] J. M. Horsfall, M. N. Horsfall & A. I. (1999). Speciation of heavy metals in intertidal sediments of the Okrika river system, Rivers State Nigeria. *Bullet Chem Soc Eth*, 13: 1-10.

[5] D. Jalija & A. Uzairu. (2020) Adsorption of Cu (II) and Ni (II) Ions from Solution onto Calcium Alginate Beads. *J. Appl. Sci. Environ. Manage*, 24 (2);329-333

[6] E. Mathew, A. Bajaj, S. M. Connelly, H. Sargsyan, F. X. Ding, A. G. Haiduczok, F. Naider & M.E. Dumont (2011) Differential interactions of fluorescent agonists and antagonists with the yeast G protein coupled receptor Ste2p. *J Mol Bio* 409 (4) 513-28

[7] J. T. Matheickal, & Q. Yu. (1999).Biosorption of cadmium (II) from aqueous solution by pretreated biomass of marine algae *Durvillaea potatorium. Water Res*. 33: 335 – 343

[8] C. M. Zvinowanda, J. O. Okonkwo, N. M. Agyei, M. V. Staden & W. Jordan (2010). Recovery of lead (II) from aqueous solution by *Zea mays* tassel biosorption. *Amer. J. Biochem. Biotechnol*. 6: 1-10

[9] C. C. Imaga & A.A. Abia (2015). Adsorption kinetics and mechanisms of Ni^{2+} sorption using carbonized and modified sorghum (*Sorghum bicolor*) hull of two pore sizes (150 μm and 250 μm): A comparative study. *International Journal of Chemical Studies*, 2(5): 59-68

[10] C. M. Ngwu, O. K. Amadi, A. C. Egwu & E. C. Lucy (2020). Sorption Studies on the Removal of Industrial Dye Aniline Yellow From Aqueous Solution Using Surfactant Modified Iron Filings, *Communication in Physical Sciences*, 6(1), 675-687

[11] N.C. Feng, X.Y. Guo, S. Liang, Y.S. Zhu & J. P. Liu (2011). Biosorption of Heavy Metals from Aqueous Solutions by Chemically Modified Orange Peel. *Journal of Hazardous Materials*, 185: 49-54.

[12] O.K. Amadi, F.K. Ekuma, C. M. Ngwu and C. H. Nwankwo. (2020). Kinetic studies on biosorption of Pb(II), Cd(II) and Ni(II) ions from aqueous solution by activated ceasar weed (*Urena lobata*) bark. *J. Chem Soc. Nigeria*, 45 (1) 63 – 69

[13] R.M. Gong, Y. Z. Sun, J. Chen, H. J. Liu H & C. Yang (2005) Effect of chemical modification on dye adsorption capacity of peanut hull. *Dyes Pigments* 67, (3); 175.

[14] M. Iqbal, A. Saeed & S.I. Zafar (2009).FTIR spectrophotometer, kinetics and adsorption isotherms modelling, ion exchange, and EDX analysis for understanding the mechanism of Cd^{2+} and Pb^{2+} removal by mango peel waste. *J. Hazard. Mater*. 1; 161-164,

[15] O. K. Amadi, G. C. Onwuasoghianya, I. A. Okoro & N. N. Ozuluonye (2020). Sorption Kinetics of Pb^{2+}, Cd^{2+} And Ni^{2+} Ions Sorption from Aqueous Medium Using Butterfly Pea (*Centrosema pubescens*) Seed Pod Powder, *Communication in Physical Sciences*, 6(2), 852-861

[16] F. K. Ekuma, O.K. Amadi & R. Eke (2019). Kinetics of Adsorption of Cd(II), Ni(II), Co(II) and Cu(II) ions from aqueous medium using carbonized biosorbent derived from Pilinut (*Canarium ovatum*) seed. A*NACHEM Journal*, 9(1):1809-1821.

[17] I.A. Okoro and O.K. Amadi (2012). The use of Okra derived cellulose biomass for the removal and recovery of Cd and Pb ions from the aqueous environment. *Chemical Science Transactions*, 1(3), 683-687.

[18] F. K. Ekuma, O. K. Amadi, C. M. Ngwu & H. Ogu (2017). Sorption Kinetics of Cr(lll), Pb(ll) and Cd(ll) ions from aqueous solution by Monkey bread (*Piliostigma thonningii)* seed pod. *Chemistry Research Journal*, 2(5):163-171.

[19] I. H. Gubbuk, R. Gup, H. Kara and M. Ersoz, M (2009). Adsorption of Cu(II) onto silica gel-immobilized Schiff base derivative, *Desalination,* 249 :1243–1248

[20] P. Antonio, K. Iha and M. E. V. Sua´rez-Iha (2007). Kinetic modeling of adsorption of di-2 pyridylketone salicyloylhydrazone on silica gel. *J. Colloid Interface Sci*. 307: 24–28

[21] V. Shrihari, S. Madhan & A. Das (2005) kinetics of phenol sorption by Raw Agrowastes. *Applied Sciences*. 6, (1), 47-50.

[22] A. S. Ferreira, A. A. Mota, A. M. Oliveira, F. I. L. Rodrigues, S. N. Pacífico, S.N., da Silva, B. T. O. Abagaro, G. D. Saraiva, A. J. R. de Castro, R. N. P. Teixeira, & V. O. S. Neto (2019). Equilibrium and Kinetic Modelling of Adsorption: Evaluating the Performance of Adsorbent in Softening Water for Irrigation and Animal Consumption, *Rev. Virtual Quim.* 11, (6), 1752-1766

[23] S. Ghosh & Goswani, U. C. (2005) Studies on adsorption behaviour of Cr(VI) onto synthetic hydrous stannic oxide. *Water S.A.* 31(4); 597-602

[24] I.A. Sengil, M. Ozacar, & H. Turkmenler (2009) Kinetic and isotherm studies of Cu(II) biosorption onto valonia tannins resin. *J. of Hazard mal* 162(2-3); 1046-1052

[25] A. A. Inyinbor, F. A. Adekola, & G. A. Olatunji. (2016). Kinetics, isotherms and thermodynamic modeling of liquid phase adsorption of Rhodamine B dye onto *Raphia hookerie* fruit epicarp, *Water Resources and Industry*, 15,14–27

[26] X.Yang & B. Al-Duri (2005) Kinetic modeling of liquid phase adsorption of reactive dyes on activated carbon. *Colloid Interface 287*, 25.

[27] O. K. Amadi, F. K. Ekuma, I. A. Okoro & C.C. Aleruchi (2019). Kinetics studies of sorption of Pb(II), Cd(II) and Ni(II) ions from aqueous solution using functionalized calopo (*Calopogonus mucunoides*) seed pod. *J. Chem Soc. Nigeria*, 44, (6), 1183 - 1190

[28] J. C. Igwe, E. C. Nwokennaya & A. A. Abia. (2005) The role of pH in heavy metal detoxification by biosorption from aqueous solution containing chelating agents. *AfricanJ.ofBio*.4,(10),1109-1112.